Technical Report

Title:

Comparison of two- and three-dimensional filtering methods to improve image quality in multiplanar reconstruction of cone-beam computed tomography

Authors:

Morihisa Sagawa[1], Yasutaka Miyoseta[1], Yoshihiko Hayakawa[1], Akira Honda[2]

Affiliations:

1. Dept. of Computer Science, Kitami Institute of Technology, Hokkaido, Japan
2. Health Administration Center, Kitami Institute of Technology, Hokkaido, Japan

The author to whom correspondence:

Yoshihiko Hayakawa

Dept. of Computer Science, Faculty of Engineering

Kitami Institute of Technology

165, Koen-cho, Kitami

Hokkaido 090-8507 JAPAN

Abstract

Objectives: Two- and three-dimensional (2D & 3D, respectively) filtering methods were examined to improve the accuracy of bone morphology depicted in dental cone-beam computed tomography (CBCT) images. An attempt to improve multiplanar reconstruction (MPR) image quality was carried out by reducing the image noise.

Methods: CBCT examinations were performed with the following principal exposure parameters: I-mode, FOV 10 cm in diameter, 120 kV, 15 mA, 0.2 mm in slice thickness, and exposure time of 10 s. 2D and 3D filtering procedures for averaging, median smoothing, and Gaussian smoothing were applied for improvement of MPR images. For comparison, 2D and 3D Laplacian sharpening for images preprocessed by Gaussian sharpening was also tested.

Results: MPR images at the midsagittal plane on the maxilla are presented. Three smoothing filters yielded improvements in slightly different ways. The Gaussian filter clearly showed moderate changes. Small but obvious differences were observed between 2D and 3D filtering. When we focused on the depiction of bone contours, the effects of these noise reduction filters seemed to be minimal in morphological bone depiction. The Laplacian filter was useful for sharpening and emphasized noise in the resulting images, in contrast to those processed by smoothing filters.

Conclusions: Various smoothing filtering methods reduced the noise on MPR images of CBCT and also functioned differently between 2D and 3D filtering matrices.

Key words: computed tomography, cone beam; digital filtration; smoothing filter

Introduction

Cone-beam computed tomography (CBCT) images are generally composed of fine and isotropic voxels and therefore show high spatial resolution. In comparison with multidetector-row computed tomography (MDCT) images, CBCT resolution is limited by the high noise due to the lower level of exposure in addition to the contrast resolution [1– 5]. As the bone structures in the maxillofacial region are complicated, reconstructed three-dimensional (3D) images are of value in clinical diagnosis. Therefore, to maximize the benefits of these characteristics, several studies of bone segmentation procedures and airway dimension measurements have been performed [6–11].

One method to improve the accuracy of tissue segmentation procedures for CBCT images is digital filtering as a post-acquisition procedure. The filtering procedure generally involves image transformation in which the output image is weighted for a specific goal. Filtering is an image-processing procedure using specific local operators, which are sometimes called local matrices. Such processing procedures are useful for image sharpening, smoothing, edge-detection, edge-enhancement, etc. Such procedures are applicable for two-dimensional (2D) images as described previously [12,13]. Usually, each pixel (or voxel) value of the output image is determined by convolution calculation with the corresponding pixel (or voxel) value and neighboring pixels (or voxels) of the input image. It is conceptually simple to extend from 2D to 3D filtering in local operators. Each pixel on a 2D image has a maximum of eight neighboring pixels, whereas each voxel on a 3D image has 26 neighboring voxels. Adaptive 2D and 3D filters have been applied to MDCT images for noise reduction and improvement of low contrast resolution [14–16]. However, 2D and 3D filters have not been applied to CBCT images.

In the present study, 3D filtering methods and the corresponding 2D filters were examined to improve both CBCT image quality and the precision of bone depiction. The whole region of interest is scanned in a single exposure in CBCT, and the images have isotropic voxels that are different from the standard anisotropic voxels in MDCT, but the effects of filter dimensions are visible. The present study was performed to examine various digital filtering procedures using 2D and 3D local operators for improvement of multiplanar reconstruction (MPR) image quality.

Materials

Image acquisition

CBCT examination was performed using CB Throne (Hitachi Medical Systems, Tokyo, Japan). Principal exposure parameters were as follows: I-mode, Field of View (FOV) 10 cm in diameter, 120 kV, 15 mA, 0.2 mm slice thickness, and 10 s exposure time [2,17,18]. The exposure dose was thought to be equivalent to those under similar exposure conditions reported for CB MercuRay (Hitachi Medical Systems) [2]. The isotropic voxels were 0.2 mm × 0.2 mm × 0.2 mm, and the individual image matrix was 512 × 512 × 512. The 3D processing and display software OsiriX (Univ. Hosp. Geneva, Switzerland) was used [19].

Filtering procedures

In general, the filtering procedure is the image transformation that the output image is weighted for a specific goal. The 2D and 3D filtering procedures of averaging, median smoothing, and Gaussian smoothing were compared. For further comparison, Gaussian smoothing followed by Laplacian sharpening was also applied.

When 2D functions *f(x, y)* and *g(x, y)* are defined as input and output images, respectively, 2D filtering procedures are expressed as follows:

$$g(x,y)=\sum_{k=-M/2}^{M/2}\sum_{l=-N/2}^{N/2} f(x+k,y+l)h(k,l) \qquad (1)$$

The function, *h(k, l)*, is a spatial filter (or local operator) with matrix size, $M \times N$. Both M and N are odd numbers. Parameters *x* and *y* are variables to indicate the pixel at the center of the spatial filter.

Similarly, the 3D filtering procedure is expressed as follows:

$$g(x,y,z)=\sum_{i=-L/2}^{L/2}\sum_{j=-M/2}^{M/2}\sum_{k=-N/2}^{N/2} f(x+i,y+j,z+k)h(i,j,k) \qquad (2)$$

f(x, y, z), *g(x, y, z)*: input and output images in three dimensions

h(i, j, k): a spatial filter (or local operator) and the matrix size is $L \times M \times N$. L, M, and N are odd numbers.

x, y, z: variables to indicate the voxel at the center of the spatial filter.

As shown in Formulas (1) and (2), the output image is calculated by summation of the product of pixel (or voxel) value and the filter value at the same pixel (or voxel) element corresponding to the center of the

spatial filter. This is the convolution integral. The calculation is repeated while the center of the spatial filter is shifted at one-pixel (or voxel) intervals. The sizes of filters examined were set at either 3 × 3 in 2D or 3 × 3 × 3 in 3D, which were the minimal sizes for the operation.

Due to the concept of the neighbor pixels (or voxels), two alternatives exist for the filtering procedures in 2D and 3D, respectively. As shown in Fig. 1, two alternatives are possible in the numbers of neighboring pixels (or voxels) to be incorporated into the calculation: four neighbors or eight neighbors in 2D filtering and six neighbors or 26 neighbors in 3D filtering. Only eight neighbors in 2D and 26 neighbors in 3D were examined in the present study.

The details of the filtering procedures are as follows:

(1) Averaging: All nine pixels (the center pixel and eight neighbors) in 2D and 27 voxels (the center pixel and 26 neighbors) in 3D have uniform weighting.

(2) Median smoothing: The value of the center pixel (or voxel) is replaced with the median value of nine pixels and 27 voxels.

(3) Gaussian smoothing: According to the Gaussian function, weighting factors are changed between the center pixel (or voxel) and either eight neighbors in 2D or 27 neighbors in 3D.

(4) Laplacian sharpening: The weighting factors are set -1 at all neighbors in 2D and 3D. The weighting factors at the center pixel and voxel are nine and 27, respectively.

Results

Effects of various filtering procedures were examined for the MPR images. The original image (top row) and processed images at the midsagittal plane are presented in Fig. 2. The processed images in the array show averaging, median smoothing, Gaussian smoothing (Sigma, standard deviation, was set at 2.0 [σ = 2.0]), and the Laplacian sharpening pre-processed by the Gaussian smoothing from the second row to the lowest row. Images processed by 2D filters are shown on the left, and those by 3D filters are on the right. Each image shows the grayscale profile along the specific vertical line, which is indicated by a vertical line and arrows. Line profiles show gray level distributions of corresponding pixels on each image. The close-up formula of processed images and profiles in Fig. 2 is shown in Fig. 3. Three arrows were added to the profiles of both the original image and the image processed by 2D and 3D Gaussian filters. Not only these profiles but also other profiles showed differences in shapes of the three peaks.

Discussion

Averaging, median smoothing, and Gaussian smoothing are noise-reduction procedures. As the matrix size for convolution with filters was the smallest, *i.e.*, 3 × 3 or 3 × 3 × 3, there seemed to be no changes in bone morphology depiction despite the clear appearance of noise reduction. Noise reduction was visible on both the image and the line profile of gray levels in Fig. 2 and Fig. 3. The Gaussian filter clearly showed moderate changes in the processed image and the profile in comparison with other smoothing filters. Gaussian smoothing was performed followed by Laplacian sharpening with good results, as shown in Fig. 3. Processing with only Laplacian sharpening was also performed, but the noise components degraded the images (data not shown).

Due to the concept of the neighbor pixel (or voxel), two alternative filtering procedures are possible in 2D and 3D, as shown in Fig. 1. Only eight neighbors in 2D and 26 neighbors in 3D were examined in the study. Four neighbors in 2D and six neighbors in 3D, in which neighboring pixels (or voxels) in the diagonal direction were omitted, were not examined. These procedures have the advantage of shortening the calculation time. However, this is unnecessary, because filters with the smallest matrix sizes of 3 × 3 or 3 × 3 × 3 for 2D and 3D, respectively, were applied. If filters with larger matrix sizes are used, it would be useful to use four neighbors in 2D and six neighbors in 3D to reduce the processing time. However, this is not practical if the original image contains relatively high levels of image noise. The loading of the calculation was higher with Gaussian smoothing than the others, and it required several minutes on a standard PC.

Images at the midsagittal plane before and after processing are shown in Figs. 2 and 3, as the difference between 2D and 3D filtering procedures was thought to appear along the superior–inferior (S–I) direction. Images and their profiles processed by averaging, median smoothing, and Gaussian smoothing showed slight differences in noise components. This was because processing by 2D filtering retained the noise component along the S–I direction.

Matrix sizes larger than 3 × 3 and 3 × 3 × 3 were not examined in this study, as large filters seemed to increase the time for calculation in 3D, and the depiction of bone morphology was reduced by excess smoothing. Applicable matrix sizes for filtering are thought to be dependent on pixel (or voxel) sizes of images, and only moderate filtering procedures were examined in the present study.

In conclusion, CBCT images are composed of fine and isotropic voxels, but the noise level is

comparatively high due to the low exposure. Therefore, there are limitations of spatial resolution. In this study, the effects of three moderate smoothing filters and a smoothing filter followed by a sharpening filter were examined. None of these procedures resulted in degradation of images of bone morphology. As 3D filtering works for smoothing along the S–I direction, resultant differences between 3D and 2D filtering procedures appeared on MPR images and their line profiles.

References

1. Baba R, Konno Y, Ueda K, Ikeda SR. Comparison of flat-panel detector and image-intensifier detector for cone-beam CT. Comput Med Imaging Graph. 2002;26:153–58.
2. Araki K, Maki K, Seki K, Sakamaki K, Harata Y, Sakaino R, *et al.* Characteristics of a newly developed dentomaxillofacial X-ray cone beam CT scanner (CB MercuRay): system configuration and physical properties. Dentomaxillofac Radiol. 2004;33:51–9.
3. Loubele M, Maes F, Schutyser F, Marchal G, Jacobs R, Suetens P. Assessment of bone segmentation quality of cone-beam CT versus multislice spiral CT: a pilot study. Oral Surg Oral Med Oral Pathol Oral Radiol Endod. 2006;102:225–34.
4. Arnheiter C, Scarfe WC, Farman AG. Trends in maxillofacial cone-beam computed tomography usage. Oral Radiol. 2006;22:80–5.
5. Shi H, Scarfe WC, Farman AG. Three-dimensional reconstruction of individual cervical vertebrae from cone-beam computed-tomography images. Am J Orthod Dentofacial Orthop. 2007;131:426–32.
6. Naitoh M, Hirukawa A, Katsumata A, Saburi K, Okumura S, Ariji E. Imaging artifact and exposure conditions in limited-volume cone-beam computed tomography: comparison between an image intensifier system and a flat panel detector. Oral Radiol. 2006;22:69–74.
7. Shi H, Scarfe WC, Farman AG. Maxillary sinus 3D segmentation and reconstruction from cone beam CT data sets. Intl J Comput Assist Radiol Surg. 2006;1:83–9.
8. Shi H, Scarfe WC, Farman AG. Upper airway segmentation and dimensions estimation from cone-beam CT image datasets. Intl J Comput Assist Radiol Surg. 2006;1:177–86.
9. Yamashina A, Tanimoto K, Sutthiprapaporn P, Hayakawa Y. The reliability of computed tomography (CT) values and dimensional measurements of the oropharyngeal region using cone beam CT: comparison with multidetector CT. Dentomaxillofac Radiol. 2008;37:245–51.
10. Yamashina A, Tanimoto K, Ohtsuka M, Nagasaki T, Sutthiprapaporn P, Iida Y, *et al.* A morphological comparison of the piriform sinuses in head-on and head-rotated views of seated subjects using cone-beam computed tomography. Oral Radiol. 2008;24:64–70.
11. Sutthiprapaporn P, Tanimoto K, Ohtsuka M, Nagasaki T, Konishi M, Iida Y, *et al.* Improved inspection of the lateral pharyngeal recess using cone-beam computed tomography in the upright position. Oral Radiol. 2008;24:71–5.

12. Analoui, M. Radiographic digital image enhancement. Part II: transform domain techniques. Dentomaxillofac Radiol. 2001;30:65–77.
13. Rosenfeld A, Kak AC. Enhancement. In: Digital Picture Processing 2nd Ed. Vol. 1. New York, NY: Academic Press, 1982;237–64.
14. Kubo T, Lin PJP, Stiller W, Takahashi M, Kauczor HU, Ohno Y, *et al.* Radiation dose reduction in chest CT: a review. Am J Roentgenol. 2008;190:335–43.
15. Kubo T, Nishino M, Kino A, Yoshimura N, Lin PJ, Takahashi M, *et al*. 3-Dimensional adaptive raw-data filter: evaluation in low dose chest multidetector-row computed tomography. J Comput Assist Tomogr. 2006;30:933–8.
16. Kalra MK, Wittram C, Maher MM, Sharma A, Avinash GB, Karau K, *et al*. Can noise reduction filters improve low-radiation-dose chest CT images? Pilot study. Radiology. 2003;228:257–64.
17. Yajima A, Otonari-Yamamoto M, Sano T, Hayakawa Y, Otonari T, Tanabe K, *et al*. Cone-beam CT (CB Throne) applied to dentomaxillofacial region. Bull Tokyo Dent Coll. 2006;47:133–41.
18. Tanabe K, Nishikawa K, Yajima A, Mizuta S, Sano T, Kousuge Y, *et al.* Suitable exposure conditions for CB Throne: New model cone beam computed tomography unit for dental use, The Shikwa Gakuho. 2008;108:104–9. (in Japanese)
19. Ratib O, Rosset A. Open-source software in medical imaging: development of OsiriX. Intl J Comput Assist Radiol Surg. 2006;1:187–96.

Figure legends

Fig. 1. Two types of alternative matrix for filtering in 2D and 3D, respectively. From left to right, each matrix has four, eight, six, and 26 neighbors to the pixel (or voxel) at the center. In this study, only eight neighbors in 2D and 26 neighbors in 3D were examined.

Fig. 2. MPR images at midsagittal plane are presented as follows. The original image (highest row) and processed images set in an array are averaging, median smoothing, Gaussian smoothing, and Gaussian smoothing followed by Laplacian sharpening (from the second row to the bottom row). The grayscale profile along the specific vertical line indicated by arrows was attached to each image. Images and profiles on the left were processed by 2D filters, and those on the right side were processed by 3D filters.

Fig. 3. Close-up of processed images and their profiles in Fig. 2. Three arrows were added to the profiles of the original image and processed images by 2D and 3D Gaussian filters.

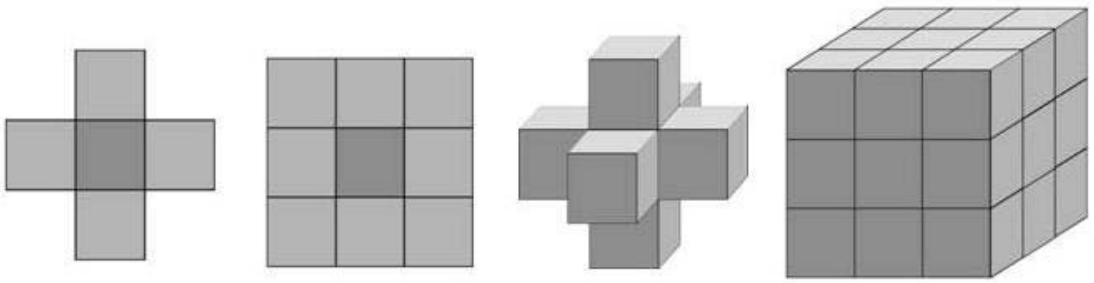

Fig. 1

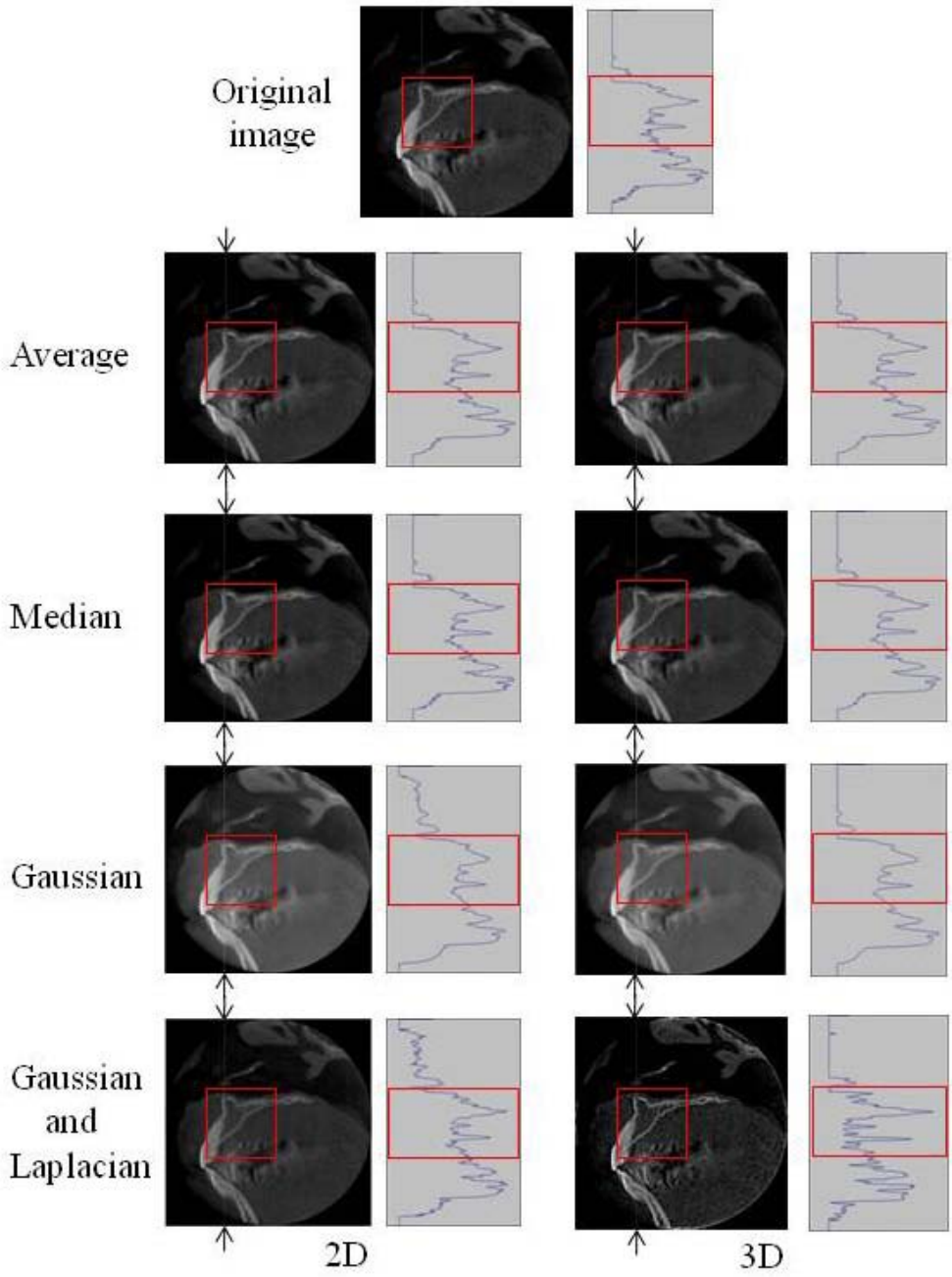
Original image
Average
Median
Gaussian
Gaussian and Laplacian
2D
3D

Fig. 2

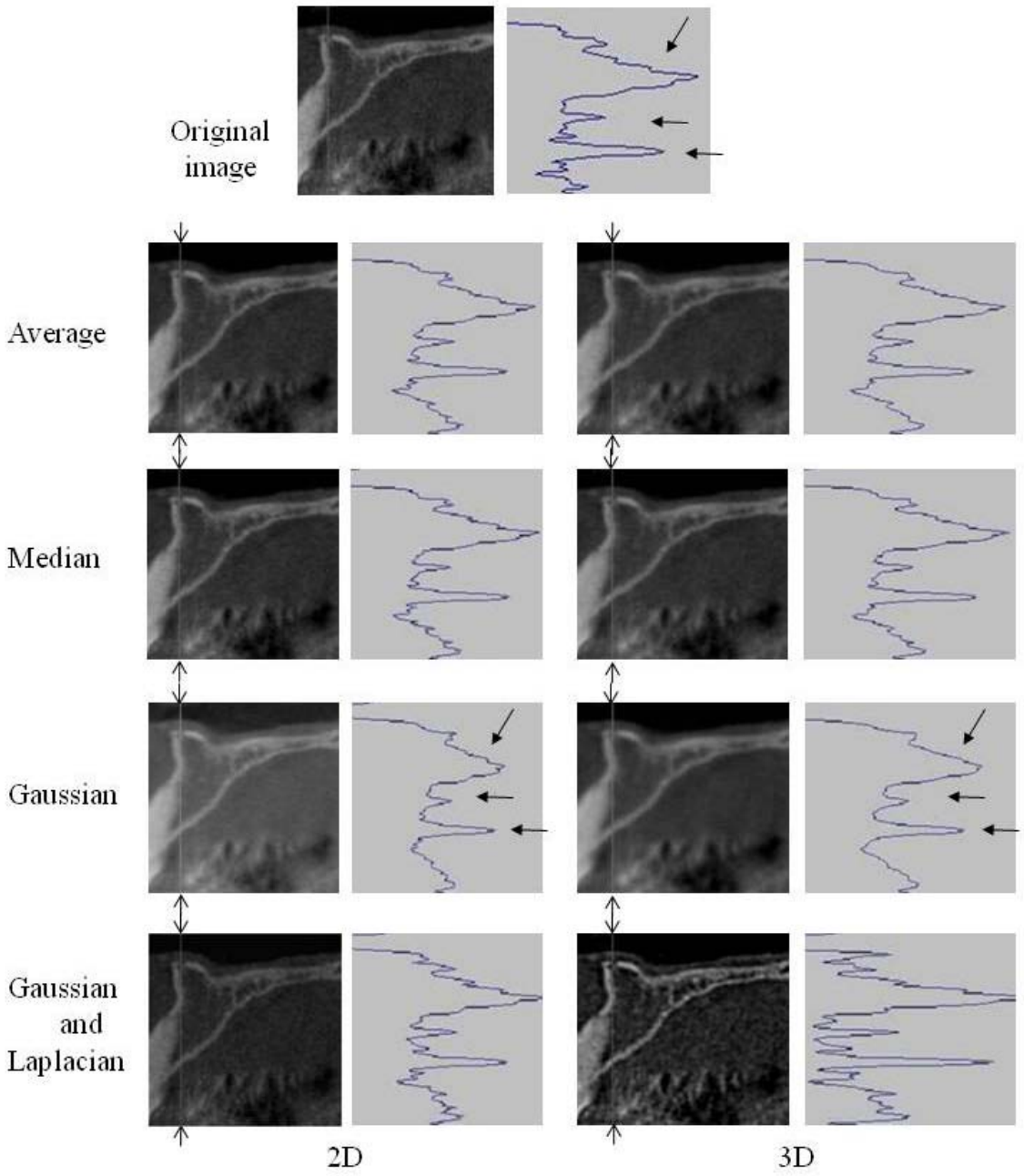
Original image
Average
Median
Gaussian
Gaussian and Laplacian
2D
3D

Fig. 3